

Eustatic sea-level change at the Mid-Pleistocene climate transition: new evidence from the shallow-marine sediment record of Japan

Akihisa Kitamura^{a,*}, Takeshi Kawagoe^b

^a*Institute of Geosciences, Faculty of Science, Shizuoka University, Shizuoka 422-8529, Japan*

^b*Kumagaigumi, Co. Ltd., 2-1, Tsukudo-Cho, Shinjuyuku, Tokyo 162-8557, Japan*

Received 23 May 2004; accepted 23 February 2005

Abstract

Based on the excellent sedimentary record, we have identified five depositional sequences in the upper part of the Omma Formation, exposed along the Japan Sea coast of central Japan. The base of this stratigraphic section is placed just below the top of the Jaramillo Subchron, and the top is located below the Brunhes-Matuyama boundary. Biostratigraphy supports the interpretation that the lower three sequences correlate with marine oxygen isotope stages (MIS) 28–26, 26–24 and 24–22, respectively. We have reconstructed a eustatic sea-level curve from analyses of sedimentary facies, fossil molluscs, basin subsidence and sediment accumulation. The resulting sea-level curve shows that mean eustatic sea-level dropped between 1.0 and 0.9 Ma, and that sea-level was lowest at MIS 22, which has the heaviest $\delta^{18}\text{O}$ value between MIS 28 and 22. The total fall in mean sea-level is inferred to be 20–30 m. This independent sea-level record demonstrates that ice-sheet volume rapidly increased at the Mid-Pleistocene Climate Transition (MPT) and culminated in MIS 22, as inferred from the $\delta^{18}\text{O}$ record. The upper two depositional sequences imply the contribution of precession to changes in ice sheet volume would have arisen in MIS 21, just after the MPT.

© 2005 Elsevier Ltd. All rights reserved.

1. Introduction

The switch from predominant 41-ka to predominant 100-ka glaciation cycles at around 1.0–0.9 Ma (the Mid-Pleistocene Climate Transition (MPT)) occurred without a corresponding change in orbital forcing (e.g., Pisias and Moore, 1981). High-resolution oxygen isotope records imply that an ice volume-related increase in mean $\delta^{18}\text{O}$ took place near the top of the Jaramillo Subchron, with a value of 0.36‰ or 0.18‰ (Prell, 1982; Maasch, 1988). According to Mudelsee and Schulz (1997), the MPT was centered at 922 ± 12 ka and lasted about 40 ± 9 ka, but the amplitude of the 100-ka cycle abruptly increased much later on, at 641 ± 9 ka. The MPT consisted of a $\delta^{18}\text{O}$ increase of 0.29 ± 0.05 ‰, which was caused by an expanding ice mass and minor

temperature effects. Raymo et al. (1997) discovered that this transition was accompanied by a 0.3‰ decrease in mean ocean $\delta^{13}\text{C}$ at the MPT and suggested that this one-time addition of isotopically depleted terrestrial carbon may possibly have been related to an increase in global aridity. Internal climatic mechanisms such as ice-bedrock interaction, atmospheric CO_2 levels, tectonic processes, and a nonlinear response to precession have been among the hypothesized causes (Raymo et al., 1988; DeBlonde and Peltier, 1991; Raymo and Ruddiman, 1992; Clark et al., 1999; Elkibbi and Rial, 2001). To solve this problem requires precise information about changes in global ice volume at the MPT. Although the history of continental ice volume comes from oxygen isotope records of foraminifera in deep-marine sediments, these records are also influenced by regional climate changes. In fact, there are differences in the pattern and amplitude of fluctuations among studies of the MPT (e.g., Mudelsee and Schulz, 1997). Direct calibration of the ice-volume component of the

*Corresponding author. Tel.: +81 54 2384798; fax: +81 54 238 0491.

E-mail address: seakita@ipc.shizuoka.ac.jp (A. Kitamura).

deep-marine oxygen isotope records with actual eustatic sea-level changes has been accomplished in studies of late Pleistocene coral-terrace sequences (e.g., Chappell et al., 1996) and submerged speleothems (e.g., Richards et al., 1994). Whether the same calibration is valid for the MPT isotopic records is unknown, because an independent calibration of the ice volume does not exist. Shelfal and nearshore sedimentary records are an independent archive of eustatic sea-level changes (Naish, 1997; Kamp and Naish, 1998). Exposures of mid-Pleistocene shallow-water sediment are known from the Wanganui Basin in New Zealand (Abbott and Carter, 1994), the Croton Basin in southern Italy (Rio et al., 1996; Massaria et al., 1999), and the San Francisco Peninsula in northern California (Carter et al., 2002). However, these authors did not identify oxygen isotope stage 23 in their lithostratigraphic schemes.

The Omma Formation is exposed in the vicinity of Kanazawa City on the Sea of Japan coast of central Japan and consists mainly of shallow-marine deposits. Its upper part occupies the interval between the top of the Jaramillo Subchron and the Matuyama/Brunhes transition (Kitamura, 1994). On the basis of litho- and biofacies, the upper part of the Omma Formation at its type section (the Okuwa section) was deposited in a variety of coastal plain, shoreface, and marine-shelf environments. Although three depositional sequences have been recognized in the upper part of the Omma Formation, and correlated with oxygen isotope stages 28–22, there is a discrepancy between these correlations and biostratigraphic data (Kitamura, 1994). However, we have gained important insights into the sequence stratigraphy of these beds by examining new exposures and evaluating drilling data associated with highway construction. As a result, we define the upper part of the Omma Formation to contain five depositional sequences and, as noted below, resolve the discrepancy in correlation between biostratigraphic and oxygen isotope ages. Further, by comparing a sea-level curve inferred from this revised sequence stratigraphic interpretation with deep-sea oxygen isotope records, we provide constraints on global sea-level changes at the MPT.

2. Geological setting of Omma Formation depositional sequences

The sedimentary basin in which the Omma Formation was deposited is a back-arc basin with respect to the subducting plate boundaries of the Pacific, Philippine and Eurasia plates (Fig. 1). The Omma Formation unconformably overlies the Middle Miocene Saikawa Formation that consists of massive siltstone (Ogasawara, 1977). Because the unconformity is penetrated by the marine rock-boring bivalve *Zirfaea* sp., the Saikawa

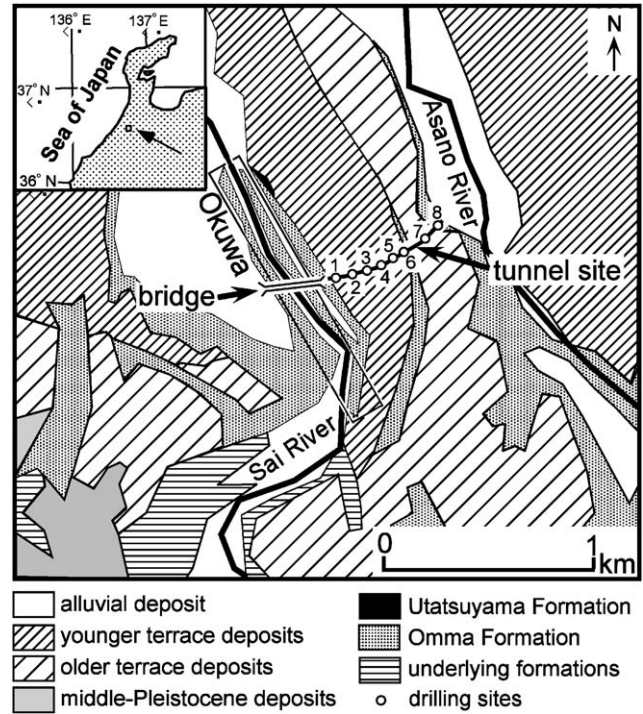


Fig. 1. Map showing tunnel, locations of cores and type section of the Omma Formation. Geologic map is modified from Imai (1959).

Formation sediments must have lithified prior to deposition of the Omma Formation (Kitamura, 1997). The sediments of the Omma Formation are poorly unconsolidated and can be easily scored with a knife. The 210-m thick Omma Formation has been divided into lower, middle and upper parts, based on its litho- and biofacies (Kitamura and Kondo, 1990). Its lower and middle parts are composed of fourteen sixth-order (41-ka) depositional sequences that were deposited in inner- to outer-shelf depths during oxygen isotope stages 56–28 (Fig. 2) (Kitamura et al., 1994, 2001). These depositional sequences include the following architectural elements, in ascending stratigraphic order: (1) a basal sequence boundary that is superposed on the ravinement surface; (2) a transgressive systems tracts (TST) (2–5 m thick) consisting of a basal shell bed (0.3 m thick) (a condensed onlap shell bed) and overlying fine- to very-fine-grained sandstone; (3) a maximum flooding horizon that coincides with the horizon that has the maximum concentration of sand-size carbonate grains; (4) a highstand systems tracts (HST) (2–3 m thick) consisting of fine-grained sandstone and sandy siltstone; and (5) a regressive systems tracts (RST) (<1 m thick) comprising fine-grained sandstone with a coarsening-upward trend (Kitamura et al., 2000). These parts of the Omma Formation show no progressive shift in litho- and biofacies toward deeper or shallower deposits. In addition, if oxygen isotope records (e.g., Ruddiman et al., 1989; Shackleton et al., 1990; Berger et al., 1994)

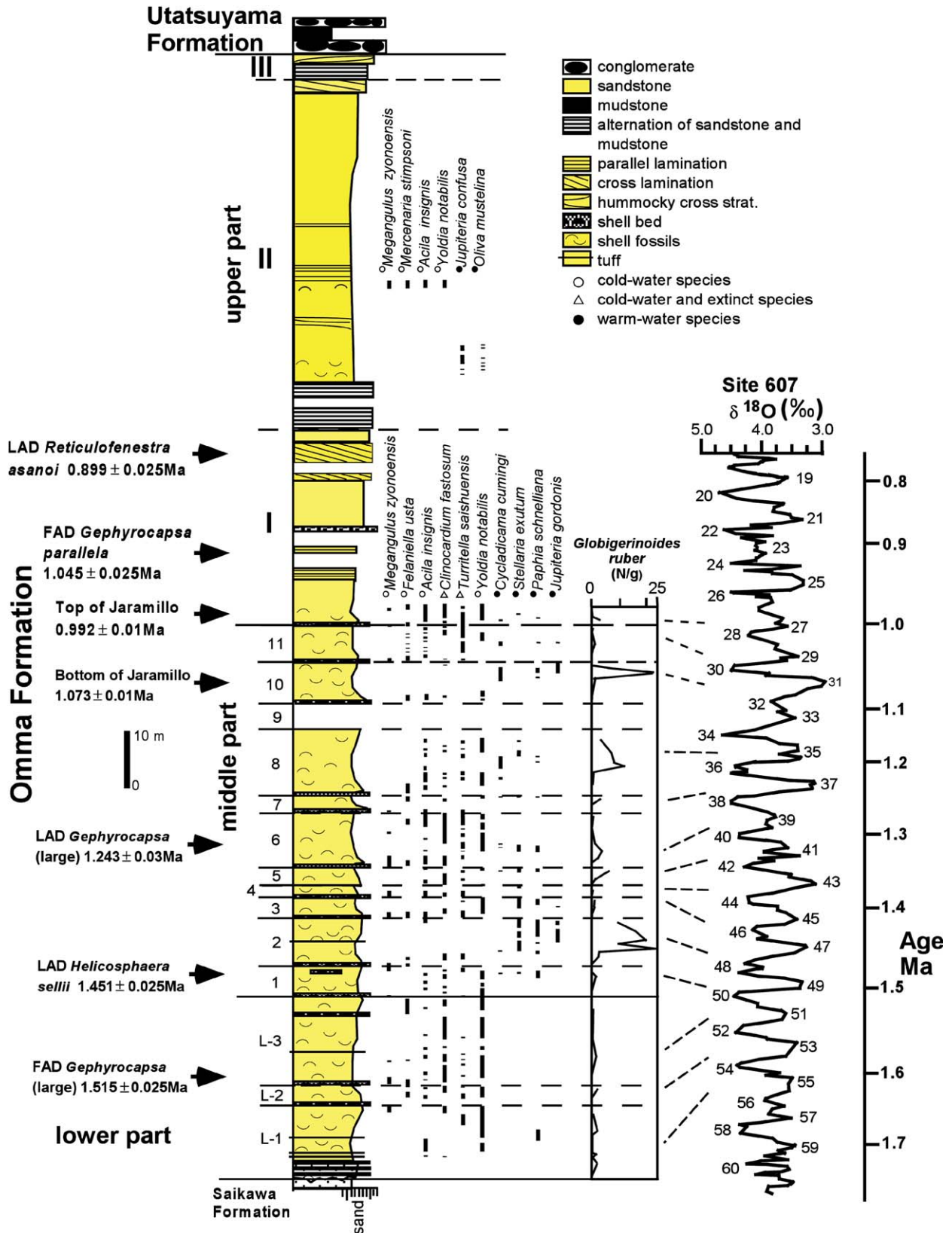


Fig. 2. Columnar section of the Omma Formation at its type section. Biostratigraphic datum horizons are after Takayama et al. (1988) and Sato and Takayama (1992); magnetostratigraphic data from Ohmura et al. (1989) and Kitamura et al. (1994); time scale for the oxygen isotope record at DSDP Site 607 and ages of biostratigraphic datum horizons and magnetic polarity changes are based on chronology of Berger et al. (1994). SB: Sequence boundary. L-1 to 3, 1–11, I–III: depositional sequence numbers.

are regarded as a proxy of the glacio-eustatic sea-level record, there were no significant changes in average sea-level during deposition of this formation. These characteristics imply that the sedimentation rate matched the subsidence rate.

The upper part of the Omma Formation is 110-m thick, has an E–W strike and dips 10° north. Based on the stack of seven sedimentary facies, this upper part is thought to consist of three depositional sequences (Kitamura, 1994), numbered from DS I to DS III (Fig. 3). Depositional sequence I (DS I) was partially covered by fluvial deposit (Fig. 2). The first-appearance datum of *Gephyrocapsa parallela* (1045 ± 25 ka; Berger et al., 1994) and the last-appearance datum of *Reticulofenestra asanoi* (889 ± 25 ka; Berger et al., 1994) have been placed within DS I (Takayama et al., 1988). A magnetostratigraphic study by Ohmura et al. (1989) inferred that the Omma Formation is assignable to the Matuyama Reversed Polarity Chron. The top of the Jaramillo Subchron is placed 65 ± 15 cm above the lower sequence boundary of DS I (Kitamura et al., 1994). Kitamura (1994) inferred that the depositional ages of DS I, II and III correspond with oxygen isotope stages 28–26, 26–24 and 24–22, respectively. However, based on the new information herein, this preliminary correlation is not in agreement with the stratigraphic position of the last-appearance datum of *R. asanoi* (Fig. 3).

3. Sedimentary facies

A new outcrop of the upper part of the Omma Formation was exposed at its type section during construction of bridge piers, and allows us to observe all of depositional sequence I. A large tunnel (663 m in length) connected to a bridge was dug into a terrace on the right bank of the Saikawa River in a E–W direction (Fig. 1). Prior to construction of the tunnel, eight cores were drilled at horizontal intervals of 50–100 m along the proposed path of the tunnel (Fig. 1). These cores correspond with the upper portion of DS I and the lower portion of DS II. In addition, we directly observed the semi-elliptic face of the tunnel (7.8 m height and 7.0 m wide) at each 1 m of drilling advance. The stratigraphic interval we studied in the tunnel corresponds with the upper portion of DS I. By relying on a combination of these new sedimentary records and published studies, we have identified seven sedimentary facies. The stratigraphic distribution of these facies is illustrated in Figs. 3 and 4.

3.1. Facies 1-inner shelf

This facies is composed of massive, bluish gray, fine-grained sandstone with abundant well-preserved fossil molluscs. Most of bivalves are conjoined, but are not in

life positions, and are mostly aligned parallel to bedding. This preservation implies that these deposits do not contain species transported *post-mortem* from other habitats, and so evidently are indigenous. These deposits occupy the lowest portion of DS I and the middle portion of DS II (Fig. 3).

Within the 4-m thick facies 1 of DS I, molluscan fossil associations change, in ascending order, from a transitional association to a *Clinocardium–Turritella* association (Kitamura et al., 1994). The former is characterized by a mix of cold-water species (e.g., *Acila insignis*, *Clinocardium fastosum* and *Yoldia notabilis*) and warm-water species (e.g., *Stellaria exutum* and *Paphia schnelliana*) (Fig. 3). This association probably lived at a depth of 20–30 to 50–60 m in a transitional environment between cold and warm water masses (Kitamura et al., 1994). The *Clinocardium–Turritella* association probably dwelled in the upper sublittoral zone from the tide mark to 50–60 m depth in a cold-water environment (Kitamura et al., 1994).

The thickness of facies 1 in DS II is about 16 m (Fig. 3), and the lower part of this facies contains numerous well-preserved fossil molluscs. This fossiliferous interval is about 7 m thick and changes upwards into unfossiliferous sandstone. The molluscan faunal associations within this fossiliferous interval change, in ascending order, from a *Raetellops–Macoma* association, to a *Macoma–Jupiteria* association (Fig. 3) (Kitamura et al., 1994). The former is characterized by *Raetellops pulchellus* and *Macoma tokyoensis*, which commonly live at depths shallower than 20–30 m in inner bays around Japan (Matsushima, 1984). The characteristic species of the latter association are *Ringicula doliaris*, *M. tokyoensis*, *Jupiteria confuse* and *Oliva mustelina*, while *Conus sieboldii*, *Pecten albicans*, *Nitidotellina hokkaidoensis* and *Panopea japonica* are also present. Based on the modern habitat of these species around Japan, this association dwells between 30 and 50 m deep in warm water (Kitamura, 1994). Molds of the large bivalves of *M. stimpsoni*, *A. insignis* and *Megangulus zyonoensis* are present in a generally unfossiliferous sandstone bed 15 m above the base of this unit (Kitamura, 1994). These species are classified as *Megangulus* association and live between the low-tide mark and 30 m depth in cold-water (Fig. 3) (Kitamura et al., 1994).

Judging from molluscan fossil associations and the near absence of physical sedimentary structures such as laminae, facies 1 is inferred to be an inner shelf deposit.

3.2. Facies 2 sand-dominated lower shoreface-inner shelf transition

This facies is subdivided into two parts. Facies 2a is characterized by brown, well-sorted, massive, medium-grained sandstone with sporadic pebbles and ichnotaxa

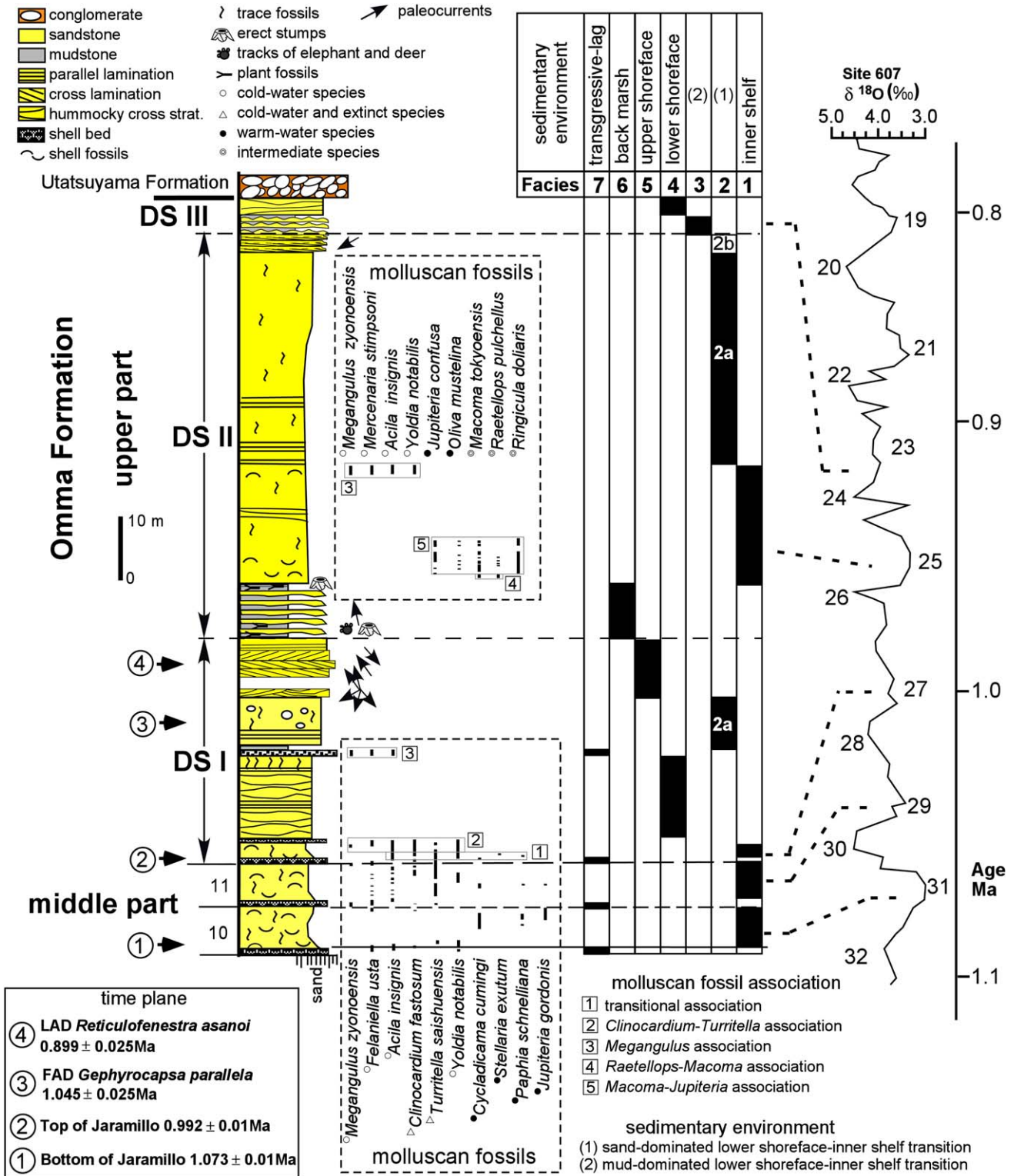


Fig. 3. Columnar section for the upper part of the Omma Formation. Note that there is a discrepancy between biostratigraphic data and oxygen isotope stages for the correlation of depositional sequences.

such as *Rosselia*. Small-scale trough lamination and low-angle hummocky cross-stratification (HCS) are common features. Fossil molluscs are rare, and are not identifiable due to dissolution of the shells. Facies 2a deposits

occupy the middle portion of DS I and the upper portion of DS II. The thicknesses of the former and latter facies are about 17 and 35 m, respectively (Figs. 3 and 4). A few individuals of the echinoid *Scaphechinus*

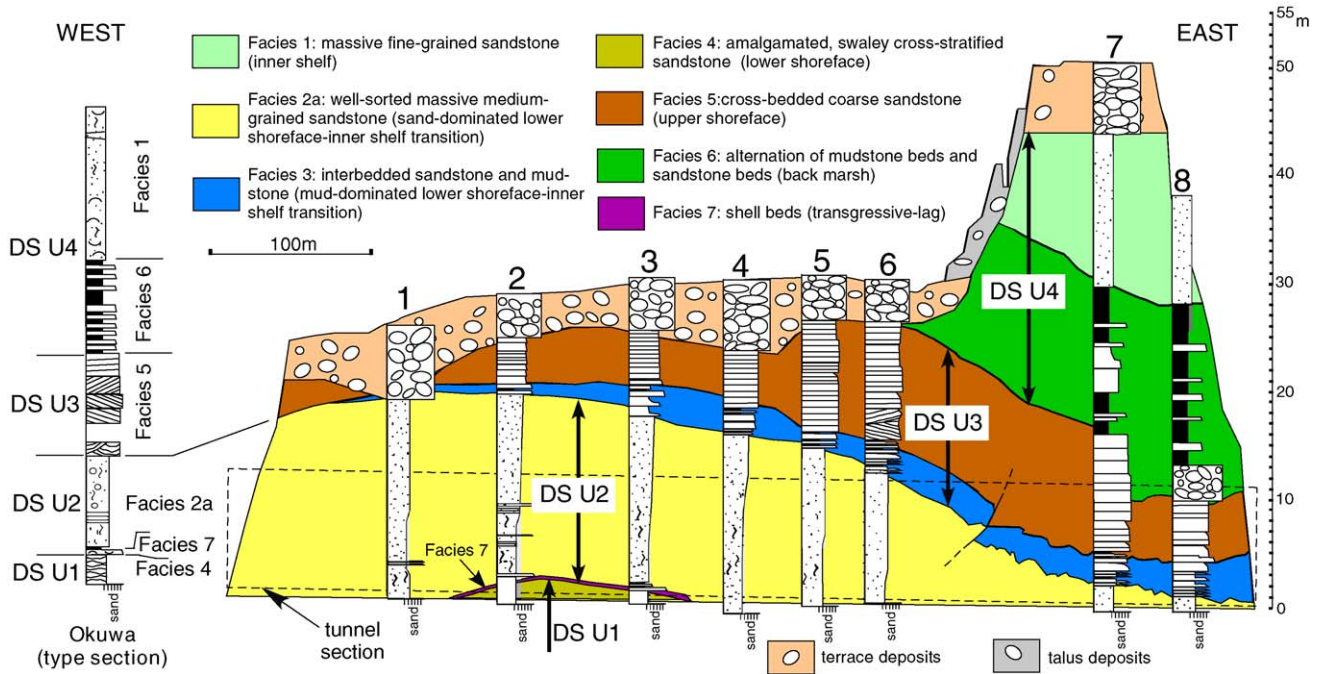


Fig. 4. Correlation panel for drill cores. See legend in Fig. 3 and text.

sp. occur in this facies in DS II. A coarsening-upward trend is evident in both horizons (Figs. 3 and 4).

Facies 2b is characterized by rhythmic 40-cm-thick graded sandstone beds with sharp erosional bases. The lower part of each bed consists of HCS or parallel- and trough cross-laminated, coarse to medium sand. Symmetrical ripple laminae are present but rare. The upper part of each bed consists of massive sandstone with *Ophiomorpha* and *echinocardium* burrows. Facies 2b is 2 m thick, is recognized in the uppermost part of DS II and overlies facies 2a (Fig. 3).

According to Hamblin and Walker (1979), parallel or swaley cross-stratification (SCS) and wave ripple-laminated sands are storm-generated sand sheets that were deposited between mean fair-weather wave base and mean storm wave base. Facies 2 is interpreted as an open-ocean, sand-dominated, shoreface-inner shelf transition deposit. Although storm-generated sand sheets are present in both facies 2a and 2b, their preservation in the latter is very good compared with the former. As a result, we believe that the depositional depth for facies 2a was greater than for facies 2b.

3.3. Facies 3 mud-dominated lower shoreface-inner shelf transition

This unit is composed of interbedded sandstone and mudstone. The sandstone beds, commonly 10–40 cm thick, are graded and have sharp bases. They also are commonly parallel-laminated and wave-ripple laminated, and rarely show SCS or minor planar cross-

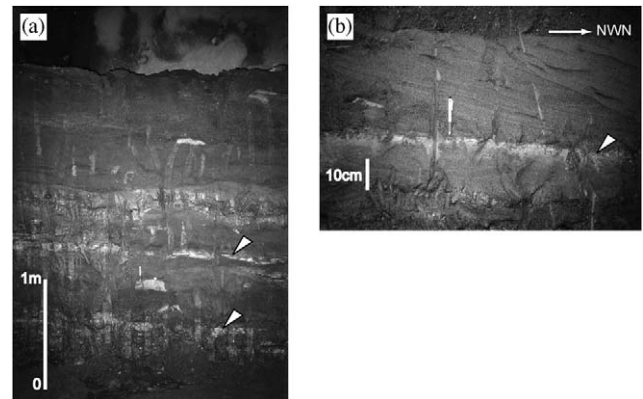


Fig. 5. Alternation of sandstone and mudstone (Facies 3) observed at the tunnel face: (a) Overview of alternation of sandstone and mudstone. Arrows show top of mudstone layers. (b) Close view showing the alternation of sandstone and mudstone.

stratification. The thickness of the massive mudstone beds is less than 10 cm. These sediments were not affected by the burrowing of benthic organisms, and this facies is present in two horizons within the upper part of the Omma Formation. The upper horizon is 2 m thick and makes up the lower portion of DS III (Fig. 3). As seen in the tunnel exposures, this facies has a lower horizon that lies within the middle portion of DS I, and it pinches out westward (<3 m thick) so that it is not present in the type section (Figs. 3–5). Coarsening- and thickening-upward trend are identified in the lower horizon (Fig. 4).

It is widely accepted that the parallel or SCS and wave ripple-laminated sands are storm-generated sand sheets deposited between mean fair-weather wave base and mean storm-wave base. In most cited examples, sand sheets are interbedded with bioturbated mudstone. However, in the present study, burrows are not present in mudstones or at the upper boundaries of sandstone sheets. This implies that the recurrence intervals of storm deposits were relatively short. Saito (1989) examined modern storm deposits in the nearshore zone (20 m depth) close to the mouths of rivers near Sendai Bay, northeast Japan, and discovered that they consist of alternations of silt and sand layers without burrowing. Saito (1989) estimated the recurrence intervals of these storm deposits at 20–100 years. Since recent sediments show the same sedimentological characteristics as facies 3, we infer that facies 3 was deposited at a shoreface-inner shelf transition off a river mouth in a bay.

3.4. Facies 4 lower shoreface

This facies is characterized by amalgamated, swaley cross-stratified, well-sorted, fine to very fine-grained sandstone, and is present in the middle portion of DS I (13 m thick) and the upper part of DS III (2 m thick) (Fig. 3). The facies is inferred to represent a lower-shoreface environment, and was deposited above mean fair-weather wave base (Bourgeois, 1980; Murakoshi and Masuda, 1992; Walker and Plint, 1992).

3.5. Facies 5 upper shoreface

Facies 5 is characterized by composite sets of high-angle, planar or trough cross-stratified, well-sorted, medium to very coarse sandstone beds. The thickness of a set is less than 1 m. Fossils were not found. The dips of the cross beds are landward, seaward or parallel to the shoreline (Fig. 3) (Kitamura, 1994). Judging from these features, Kitamura (1994) interpreted this facies as an upper shoreface. This facies occupies the uppermost part of DS I and is less than 12 m thick (Figs. 3 and 4).

3.6. Facies 6 back marsh

This unit is composed of alternating massive mudstone beds and coarse-grained sandstone beds, with individual beds ranging from 10 to 100 cm thick (Fig. 3). The sandstone beds are graded, with erosional bases. Small-scale trough lamination is often recognized within the sandstone beds. Although most mudstone beds are massive, parallel lamination is present in a few beds. Plant debris is common in the mudstone, and erect stumps have been found in the lowermost (Kitamura and Kondo, 1990) and the uppermost (Takayama et al., 1988) mudstone beds (Fig. 3). The tracks of elephants

and deers have been found on mudstone bedding planes (Matsuura, 1996). A 3-m-thick conglomerate bed is present at the base of back-marsh deposits on the east side of the study section (Fig. 4), and consists of clast-imbricated pebble gravels. The dip of the imbrication indicates that direction of paleo-flow was to the northwest (present seaward).

The occurrence of erect stumps and land mammal tracks indicates that the sediment of this unit was subaerially exposed. The sandstone beds are thin and graded, with sharp bases. These sedimentary features are simply the products of episodic decelerating flows. In a continental context, the sedimentary environment of this alternation may be interpreted as back marsh deposits, whereas the sandstone beds can be interpreted as a flood deposit in crevasse splays. This facies is present in the lower portion of DS II and is 10 m thick.

3.7. Facies 7 transgressive lag

The facies is characterized by 20-cm-thick shell beds with erosional surfaces, and a fining-upward trend in the matrix. This facies is found from the bases of facies 1 and 2a within DS I, respectively (Fig. 3). The upper shell bed is covered by a 30-cm-thick massive siltstone.

These shell beds consist of *M. zyonoensis*, *A. insignis*, *Glycymeris yessoensis* and *Mizuhopecten yessoensis yokoyamae* (Kitamura, 1994). These shells are absent in sediment immediately below the shell beds, so are unlikely to have been reworked from older deposits. In the upper shell bed, the underlying amalgamated and SCS very fine sandstone do not contain fossils of molluscs or other macroinvertebrates. These molluscs inhabit well-sorted sandy bottoms between the low-tide mark and a depth of 30 m in cold water (Kitamura et al., 1994). Most molluscs in this facies do not show abrasion, damage due to *Cliona* boring, or encrustation by calcareous algae, barnacles or bryozoans. These characteristics are not consistent with a general model of shell accumulation resulting from low sedimentation rates. Because the molluscan fossil associations change from a cold-water association in the lower shell bed to a transitional association in overlying facies 1, this shell bed may have formed during a deglacial period. As noted below, the upper shell bed also exhibit evidence of a deepening-upward trend. We concluded that this facies is transgressive lag formed by coastal shoreface erosion.

4. Depositional sequences

Kitamura (1994) showed that the upper part of the Omma Formation consists of three depositional sequences. In the present study, we have divided the lowest of these sequences (DS I) into three depositional sequences, based on new information about lithofacies

distribution (Fig. 4). As a result, the upper part of the Omma Formation is now interpreted as consisting of five sequences (Fig. 6).

Depositional sequence U1 (DS U1) is 17 m thick and consists of the following facies, in ascending stratigraphic order: basal shell bed (Facies 7, transgressive lag), massive fine-grained sandstone with abundant molluscan fossils (Facies 1, inner shelf) and amalgamated SCS fine to very fine-grained sandstone (Facies 4, lower shoreface) (Fig. 6). The erosional base of the basal shell bed is also the lower sequence boundary and coincides with a ravinement surface formed by coastal shoreface erosion during a transgression (Bruun, 1962). Warm-water molluscs in the transitional association imply that the lower part of the massive fine-grained sandstone was deposited during an interglacial period.

Thus, we regard the massive sandstone with this association and the underlying shell bed as a TST. Inner-shelf, massive sandstone is directly overlain by a lower-shoreface SCS sandstone. This indicates that sediments of the lower shoreface-inner shelf transition were eliminated. The base of the SCS sandstone is sharp and overlain by a 20-cm-thick granule-gravel bed (Kitamura, 1994). Such a sharp-based shoreface succession has been reported from many areas (e.g., Plint, 1988, 1991; Plint and Norris, 1991). The base of the SCS sandstone is believed to have formed by wave scour during a sea-level fall (Posamentier et al., 1992). The sediment above the erosional base is defined as a falling stage systems tract (FSST) (Plint and Nummedal, 2000). Thus, we think that the SCS sandstone and the underlying massive sandstone with the cold-water

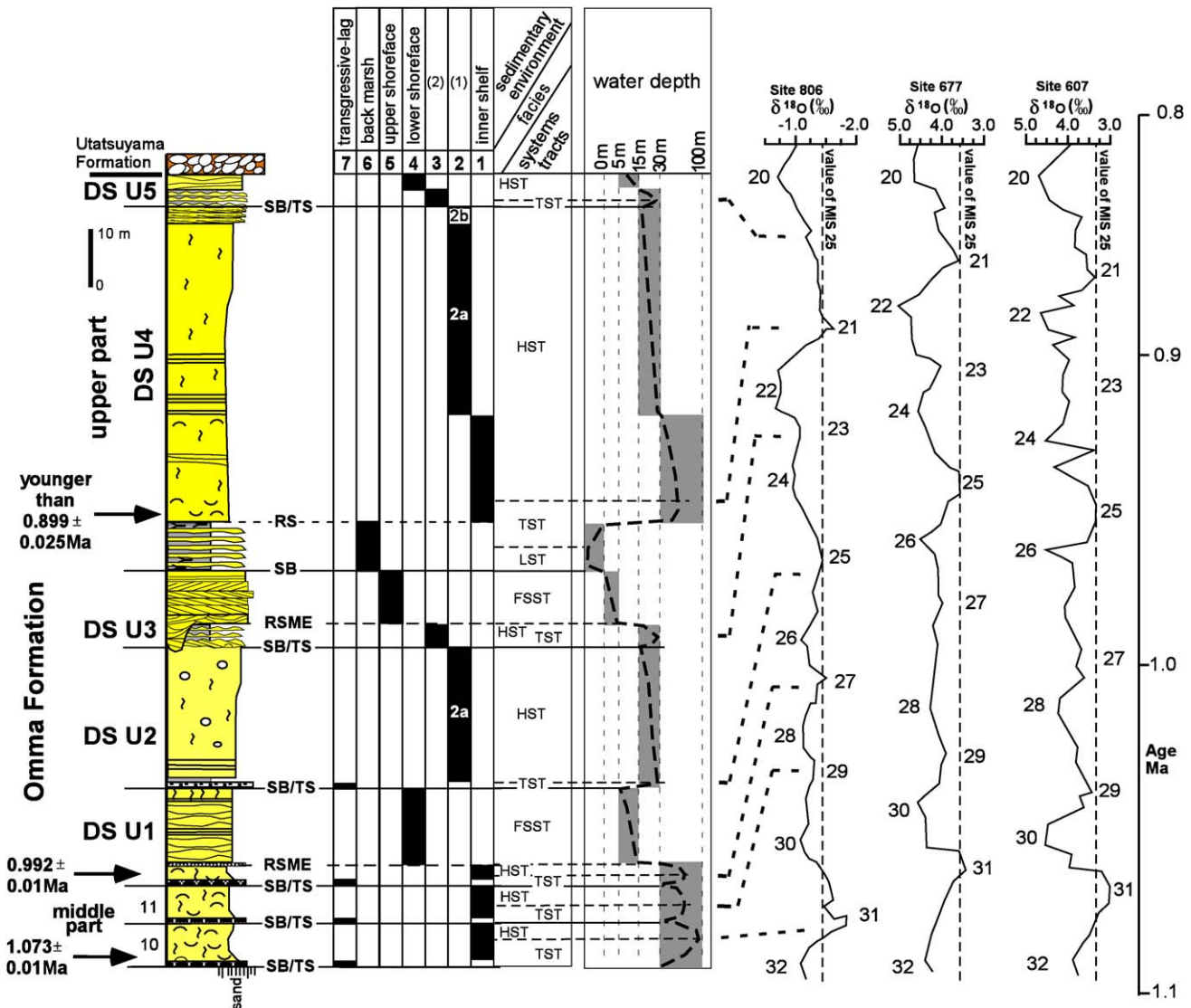


Fig. 6. Sequence stratigraphic interpretation and comparison of eustatic sea-level curve derived from sedimentary record in the upper part of the Omma Formation, with oxygen isotope records from sites 607, 677 and 806 (Ruddiman et al., 1989; Shackleton et al., 1990; Berger et al., 1994). See legend in Fig. 3.

Clinocardium–Turritella association correspond with an FSST and an HST, respectively (Fig. 6).

Depositional sequence U2 (DS U2) has a maximum thickness of 17 m and commences with a 20-cm-thick shell bed (Facies 7, transgressive-lag) resting on a sharp erosional surface and being overlain by a 20-cm-thick mudstone sheet (Fig. 6). The presence of mudstone sheet indicates that shell bed deposited below fair-weather wave base. Since the sediment below the shell bed is lower-shoreface SCS sandstone, the shell bed can be interpreted as transgressive lag formed by coastal erosion. Its base is also the lower sequence boundary and superposed the ravinement surface. A well-sorted, massive, medium-grained sandstone lies above the basal shell bed and exhibits a coarsening-upward trend (Facies 2a, sand-dominated lower shoreface-inner shelf transition) (Fig. 4). Therefore, we infer that the sandstone corresponds to an HST. In the case of all fourteen depositional sequences in the lower and middle parts of the Omma Formation, it is not possible to identify a maximum flooding surface without examining the stratigraphic distribution of planktonic foraminiferal abundance and/or fossil molluscs (Kitamura, 1998; Kitamura et al., 2001). Shells of both micro- and macrofossils in DS U2 have been dissolved, so we were unable to identify the HST base. We regard the basal shell bed and the overlying deposits as the TST and HST, respectively.

The well-preserved depositional sequence U3 (DS U3) is exposed within the tunnel. The sequence is 13 m thick, and comprises interbedded sandstone and mudstone (Facies 3, mud-dominated lower shoreface-inner shelf transition) and cross-stratified, well-sorted, medium to very coarse sandstone (Facies 5, upper shoreface) (Figs. 4 and 6). The stacking pattern from the well-sorted, massive sandstone (HST) in DS U2 to the present interbedded sandstone and mudstone implies that the depositional environment drastically changed from a sand-dominated to a mud-dominated shelf. Because this stacking pattern cannot be explained as a regressive setting, we believe that the sharp erosional base of the interbedded sandstone and mudstone is an unconformity and sequence boundary. The Facies 3 sediment represents coarsening- and thickening-upward trends for the sandstone beds, which we interpret as a TST and HST. This unit is directly overlain by the upper-shoreface sandstone. This means that the lower-shoreface zone has been eliminated, and that the upper-shoreface sandstone corresponds with the FSST, whose base represents a regressive surface of marine erosion (RSME, Plint, 1988; Hart and Long, 1996). Thus, this sequence mainly consists of an upward-shoaling facies succession and is regarded as a parasequence. Our observations suggest that the degree of erosion during formation of the RSME was greater to the westward (Fig. 6), where the lower shoreface-inner shelf transition

sediments were completely truncated at the bed along Saikawa River. Thus, DS U3 in this section contains only the FSST that comprises a progradational upper-shoreface facies (Fig. 4). This caused the misidentification of depositional sequences in DS I as presented by Kitamura (1994). The degree of preservation in DS U3 suggests that water depth increased eastward. This is consistent with reconstructions based on fossil molluscs in the middle part of the Omma Formation (Kitamura et al., 1997).

Depositional sequence U4 (DS U4) corresponds with depositional sequence II in Kitamura (1994). In this 55-m-thick sequence, the lithofacies are, in ascending order, an alternation of massive mudstone beds and coarse-grained sandstone beds (Facies 6, back marsh), massive bluish gray fine-grained sandstone (Facies 1–Inner shelf), well-sorted, massive, medium-grained sandstone (Facies 2a, lower shoreface-inner shelf transition), and rhythmic graded sandstone beds (Facies 2b, lower shoreface-inner shelf transition) (Fig. 6). Based on relative sea-level change inferred from the stacking pattern of these lithofacies, Kitamura (1994) thought that the base and top of back-marsh deposits correspond with a lower sequence boundary and a ravinement surface, respectively. In such a case, back-marsh deposits are interpreted to represent a low system tract and early TST deposits. The changes of molluscan fossil associations in the inner-shelf deposits indicate that the marine climate became warm and then cooled. In glacial-eustatic terms, sea-level is relative high during warm interglacial periods. Therefore, Kitamura (1994) placed the maximum flooding surface, which is the boundary between the TST and HST, at the midpoint of the horizon containing warm-water molluscs.

Depositional sequence U5 (DS U5) coincides with depositional sequence III of Kitamura (1994), and is composed of interbedded sandstone and mudstone (Facies 3, mud-dominated lower shoreface-inner shelf transition) and amalgamated SCS fine to very fine sandstone (Facies 4, lower shoreface) (Fig. 6). This facies succession has been reported from wave-dominated and gradationally based shoreface successions (e.g., Heward, 1981; MuCubbin, 1982). Such successions typically begin with outer-middle shelf, bioturbated mudstone. Therefore, the stacking pattern from the sandstone in the uppermost part of DS U4 to the overlying interbedded sandstone and mudstone cannot be explained by a progradational inner-shelf to shore-facies assemblage. We conclude that the sharp boundary between them corresponds to a sequence boundary. Kitamura (1994) tentatively placed the base of the HST at the midpoint of interbedded sandstone and mudstone, because these sediments do not exhibit systematic changes such as fining-upward or thickening-upward trends.

5. Discussion

We first correlated depositional sequences in the upper part of the Omma Formation with oxygen isotope records (Fig. 6). As noted above, the top of the Jaramillo Subchron is placed just above the basal shell bed in DS U1. Thus, the TST sediment in this sequence was deposited during a deglacial sea-level rise in MIS 28 to 27. According to Takayama et al. (1988) and Sato and Takayama (1992), *Gephyrocapsa parallela* is only found from inner-shelf sandstone in DS U4, whereas *R. asanoi* does not occur in the sandstone in DS U4. This implies that the sea-level highstand during the deposition of DS U4 is younger than the last-appearance datum of *R. asanoi* (889 ± 25 ka). Furthermore, the top of the Omma Formation is younger than the Matuyama/Brunhes transition (790 ± 5 ka; Berger et al., 1994) (Ohmura et al., 1989). From these observations, the depositional age of the inner-shelf sandstone in DS U4 correlates with either MIS 23 or 21. Deep-sea $\delta^{18}\text{O}$ records for sites 607, 677 and 806 (Ruddiman et al., 1989; Shackleton et al., 1990; Berger et al., 1994) show that the values for MIS 22 is significantly heavier than those for MIS 26 and 24. In addition, the duration of MIS 22–20 seems to have been 70–78 ka (Shackleton et al., 1990; Bassinot et al., 1994; Berger et al., 1994). Since DS U4 is anomalously thick and only includes non-marine sediments in its lowest portion, we believe that this sequence corresponds to MIS 22–20, and that DS U2 and U3 correlate with MIS 26–24 and MIS 24–22, respectively (Fig. 6). If this correlation is correct, then DS U5 may represent “interstadial” oscillations in sea level during the glaciation from MIS 21 to 20 (see below).

We evaluated water depth based on facies successions and molluscan fossil associations in the five depositional sequences within the upper part of the Omma Formation. Because fair-weather wave base lies at depths of about 5–15 m (Walker and Plint, 1992), the maximum depths of the lower and upper shoreface are inferred to be 15 and 5 m, respectively. Based on the bathymetric ranges of molluscan fossil associations, the minimum water depth for the inner-shelf deposits is inferred to be 30 m. A water-depth curve plotted against time, derived from the above-noted correlation between depositional sequences and oxygen isotope stages, is shown in Fig. 6.

Kitamura et al. (1994) showed that water depth changed from 20–30 to 100–120 m during depositional sequences 10 and 11 (MIS 32–28) in the middle part of the Omma Formation. These sequences do not include sediments that were deposited shallower than the inner shelf. However, the upper part of the Omma Formation mainly consists of deposits shallower than 30 m (96.4 m of 116.4 m in thickness, 83%). This implies that mean water depth decreased from 1.0 Ma (just above the top

of the Jaramillo Subchron) to 0.9 Ma (MIS 22). The total decrease in water depth is inferred to be 20–30 m. This value is a minimum estimate, because of remaining uncertainty about sea level during the deposition of back-marsh sediments in MIS 22, and about the lowstand strata lost at the bounding unconformities.

Water-depth changes were influenced by basement subsidence, sediment supply and eustatic sea-level change. The aggradational stacking pattern of deposits in the lower and middle parts of the Omma Formation suggests that sedimentation kept pace with basin subsidence at 600 ka (MIS 56–28). There are no reports of local tectonic movement in the study area during deposition of the Omma Formation. In addition, we were unable to identify differences in the mineral composition or in relative abundances of fossil molluscs within the massive sandstone that lies between the middle and upper parts of this formation (Facies 1). It is, therefore, reasonable to think that the sedimentation rate also matched the subsidence rate during deposition in the upper part of the Omma Formation. In addition, the effects of local isostasy may not have changed. Based on correlations between depositional sequences with oxygen isotope stages, the sedimentary ratios of depositional sequences 10 and 11 are estimated to be 18.8 and 27.6 cm/ka, respectively. On the other hand, the apparent rates of sediment accumulation in depositional sequences U1, U2 and U3 are 36 to 42 cm/ka. Such a difference in sedimentation rates between the middle and upper parts of the Omma Formation resulted from a drop in mean water depth.

The water-depth curve can also be affected by compaction due to water and sediment loading. The basement rock for the Omma Formation had already been consolidated prior to deposition of this formation (Kitamura, 1997). The Omma Formation mainly consists of very fine-to-fine grained sandstone, with their maximum burial depth equal to the thickness (210 m) of the Omma Formation. Based on the porosity-depth relationship (Sclater and Christie, 1980; Ramm and Bjørlykke, 1994), sandstone porosity decreases only 5% between the surface and a burial depth of 250 m. As a result, the water-depth curve was hardly influenced by the effects of compaction. The sum of these factors suggests that a decrease in mean water depth of 20–30 m was caused by global sea-level fall (Fig. 6).

Prell (1982) and Maasch (1988) documented a rapid increase in mean $\delta^{18}\text{O}$ composition of 0.36‰ or 0.18‰ near the top of the Jaramillo Subchron. These values equate to a sea-level fall of about 33 m and 16 m, respectively. More recently, Mudelsee and Schulz (1997) suggested that the MPT represents a $\delta^{18}\text{O}$ increase of 0.29 ± 0.05 ‰ (= 23 ± 5 m, sea-level fall) and was caused by an expanding ice mass. These values are very close to the change in mean water depth recorded in the Omma Formation.

Based on a comparison of maximum water depth in each depositional sequence, sea-level during MIS 23 was lower than during MIS 27, 25 or 21 (Fig. 6), which is consistent with many published $\delta^{18}\text{O}$ records (Site 607, Ruddiman et al., 1989; Site 677, Shackleton et al., 1990; Site 806, Berger et al., 1994). On the other hand, there is a difference in the $\delta^{18}\text{O}$ values between stages 25 and 27. The value for stage 25 is 0.3–0.4‰ lower than for stage 27 in $\delta^{18}\text{O}$ records for Sites 607 and 677, while both values are nearly the same at site 806. If the entire difference in $\delta^{18}\text{O}$ values contribute to ice-volume change, sea level during stage 25 was 27–36 m higher than during stage 27, based on 0.011‰ $\delta^{18}\text{O}$ for each metre of sea-level change. This water-depth value is not consistent with our curve, which incorporates uncertainty about water depth by using analyses of sedimentary facies and mollusc fossils (Fig. 6). In addition, the $\delta^{18}\text{O}$ value for stage 21 is slightly heavy relative to stage 25 at Sites 607 and 677, while the former is 0.1‰ lighter than that of the latter in Site 806. Our reconstructed a maximum water depth in each depositional sequence is consistent with the oxygen isotope record at Site 806. We therefore believe that oxygen isotope record of *G. sacculifer* from the Ontong Java Plateau (ODP Site 806; Berger et al., 1994) is most faithful record of sea-level fluctuations at the MPT. However, our generated curve indicates that the amplitude of sea-level fluctuation for each depositional sequence is significantly smaller than at Site 806 (calibration of $\delta^{18}\text{O}$ records using 0.011‰ per metre). There are at least two possible causes for this discordance. First, we do not know what the sea level was during deposition of the back-marsh sediments and lowstand strata lost at the bounding unconformities. Our estimates of water depths are therefore regarded as minimum values. Second, the $\delta^{18}\text{O}$ record at Site 806 was also influenced by regional climate change. Many studies have noted that average sea-surface temperature during the last glacial maximum was only 1–2 °C lower than in the modern western Pacific (Broecker, 1986; Trend-Staid and Prell, 2002). However, the magnesium/calcium ratio of *G. ruber* at Site 806 indicates a surface temperature was 3 °C colder than present during the last glacial maximum (Lea et al., 2000). In this latter case, the glacial–interglacial $\delta^{18}\text{O}$ amplitude at the site would be larger than that due to ice-volume changes.

It is noteworthy that DS U5 represents a sea-level oscillation in stage 21 (Fig. 6). The DS U4 horizon exhibiting maximum water depth is a massive, inner shelf sandstone, whereas in DS U5 this horizon consists of lower shoreface-inner shelf transition sediments. This means that the peak sea-level highstand during DS U5 was lower than in DS U4. According to Bassinot et al. (1994), a high-resolution oxygen isotope record from core MD900963, in which precession-related oscillations of $\delta^{18}\text{O}$ are particularly well expressed, was caused by

superposition of a local salinity signal over the global ice volume signal, and shows three precessional oscillations. The ice-volume curve of Bassinot et al. (1994) shows that ice volume was reduced in the latter interstadial periods. Thus, we conclude that the horizons with maximum water depth in DS U4 and U5 correspond with stages 21.5 and 21.3, respectively. This implies that the precession contribution to sea-level variability was stronger MIS 21.

6. Conclusions

We identified five depositional sequences in the upper part of the Pleistocene Omma Formation, based on the excellent sedimentary record at new exposures and in drilling cores associated with highway construction. When these results are combined with published biostratigraphic and magnetostratigraphic data, we conclude that the lower three depositional sequences correlate with MIS 28–22, which clearly experienced obliquity-related climate cycles. On the other hand, the upper two depositional sequences in the Omma Formation correspond with MIS 21.5 and 21.3, respectively. Our resulting eustatic sea-level curve, based on analyses of lithofacies, fossil molluscs and subsidence, indicates that a fall in eustatic sea-level of 20–30 m took place from MIS 28 to 22 (1.0–0.9 Ma). This result is in excellent agreement with the sea-level fall inferred from the $\delta^{18}\text{O}$ record. Thus, the rapid growth of ice sheets at the mid-Pleistocene transition is confirmed by the shallow-marine record in the Omma Formation. In addition, the upper two depositional sequences in the Omma Formation imply that the precessional contribution to the formation and demise of continental ice sheets was already in evidence at MIS 21, just after MPT.

Acknowledgments

We thank the late Dr. Y. Kaseno, emeritus Professor at Kanazawa University, for his helpful comments on our study. We acknowledge Prof. Ishikawa Ken-O General Public Works Office for opportunity of observation of the tunnel.

References

- Abbott, S.T., Carter, R.M., 1994. The sequence architecture of mid-Pleistocene (0.35–0.95 Ma) cyclothem from New Zealand: facies development during a period of orbital control on sea-level cyclicity. In: de Boer, P.L., Smith, D.G. (Eds.), *Orbital Forcing and Cyclic Sequences*. International Association of Sedimentologist Special Publication, vol. 19. pp. 367–394.
- Bassinot, F.C., Labeyrie, L.D., Vincent, E., Quidelleur, X., Shackleton, N.J., Lancelot, Y., 1994. The astronomical theory of climate and the

- age of the Brunhes–Matuyama magnetic reversal. *Earth and Planetary Science Letters* 126, 91–108.
- Berger, W.H., Yasuda, M.K., Bickert, T., Wefer, G., Takayama, T., 1994. Quaternary time scale for the Ontong Java Plateau: Milankovitch template for Ocean Drilling Program Site 806. *Geology* 22, 463–467.
- Bourgeois, J., 1980. A transgressive shelf sequence exhibiting hummocky cross stratification: the Cape Sebastian Sandstone (Upper Cretaceous), southwestern Oregon. *Journal of Sedimentary Petrology* 50, 681–702.
- Broecker, W.S., 1986. Oxygen isotope constraints on surface ocean temperature. *Quaternary Research* 26, 121–134.
- Bruun, P., 1962. Sea level rise as a cause of shoreface erosion. *Journal of the Waterways and Harbors Division: proceedings of the American Society of Civil Engineers* 88, 117–130.
- Carter, R.M., Abbott, S.T., Graham, I.J., Naish, T.R., Gammon, P.R., 2002. The middle Pleistocene Merced-2 and -3 sequences from Ocean Beach, San Francisco. *Sedimentary Geology* 153, 23–41.
- Chappell, J., Omura, A., Esat, T., McCulloch, M., Pandolfi, J., Ota, Y., Pillans, B., 1996. Reconciliation of late Quaternary sea levels from coral terraces at Huon Peninsula with deep sea oxygen isotope records. *Earth and Planetary Science Letters* 141, 227–236.
- Clark, P.U., Alley, R.B., Pollard, D., 1999. Northern Hemisphere ice sheet influences on global climate change. *Science* 286, 1104–1111.
- DeBlonde, G., Peltier, W.R., 1991. A one-dimensional model of continental ice volume fluctuations through the Pleistocene: implications for the origin of the mid-Pleistocene climate transition. *Journal of Climate* 4, 318–344.
- Elkibbi, M., Rial, J.A., 2001. An outsider's review of the astronomical theory of the climate: is the eccentricity-driven insolation the main driver of the ice ages? *Earth-Science Reviews* 56, 161–177.
- Hamblin, A.P., Walker, R.G., 1979. Storm-dominated shallow marine deposits; the Fernie-Kootenay (Jurassic) transition, southern Rocky Mountains. *Canadian Journal of Earth Sciences* 16, 1673–1690.
- Hart, B.S., Long, B.F., 1996. Forced regressions and lowstand deltas: Holocene Canadian examples. *Journal of Sedimentary Research*, A 66, 820–829.
- Heward, A.P., 1981. A review of wave-dominated clastic shoreline deposits. *Earth-Science Reviews* 17, 223–276.
- Imai, I., 1959. Geological map of Kanazawa District (1:50,000): Geological Survey of Japan [Japanese with English abstract].
- Kamp, P.J.J., Naish, T., 1998. Forward modeling of the sequence stratigraphic architecture of shelf cyclothem: application to late Pliocene sequences, Wanganui Basin (New Zealand). *Sedimentary Geology* 116, 57–80.
- Kitamura, A., 1994. Depositional sequences caused by glacio-eustatic sea-level changes in the upper part of the early Pleistocene Omma Formation. *The Journal of the Geological Society of Japan* 100, 463–476 (Japanese with English abstract).
- Kitamura, A., 1997. The lower unconformity and molluscan fossils of the basal part of the early Pleistocene Omma Formation at its type section, Ishikawa Prefecture, central Japan. *The Journal of the Geological Society of Japan* 103, 763–769 (Japanese with English abstract).
- Kitamura, A., 1998. Glaucony and carbonate grains as indicators of the condensed section: Omma Formation, Japan. *Sedimentary Geology* 122, 151–163.
- Kitamura, A., Kondo, Y., 1990. Cyclic change of sediments and molluscan fossil associations caused by glacio-eustatic sea-level changes during the early Pleistocene—a case study of the middle part of the Omma Formation at the type locality. *The Journal of the Geological Society of Japan* 96, 19–36 (Japanese with English abstract).
- Kitamura, A., Kondo, Y., Sakai, H., Horii, M., 1994. Fourty-one thousand-year orbital obliquity expressed as cyclic changes in lithofacies and molluscan content, early Pleistocene Omma Formation, central Japan. *Palaeogeography, Palaeoclimatology, Palaeoecology* 112, 345–361.
- Kitamura, A., Kimoto, K., Takayama, T., 1997. Reconstruction of the thickness of the Tsushima Current in the Japan Sea during the Quaternary from molluscan fossils. *Palaeogeography, Palaeoclimatology, Palaeoecology* 135, 51–69.
- Kitamura, A., Matsui, H., Oda, M., 2000. Constraints on the timing of systems tract development with respect to sixth-order (41 ka) sea-level changes: an example from the Pleistocene Omma Formation, Sea of Japan. *Sedimentary Geology* 131, 67–76.
- Kitamura, A., Takano, O., Takada, H., Omote, H., 2001. Late Pliocene-early Pleistocene paleoceanographic evolution of the Sea of Japan. *Palaeogeography, Palaeoclimatology, Palaeoecology* 172, 81–98.
- Lea, D.W., Pak, D.W., Spere, H.J., 2000. Climate impact of Late Quaternary equatorial Pacific Sea surface temperature variations. *Science* 289, 1719–1724.
- Maasch, K.A., 1988. Statistical detection of Pleistocene climate. *Climate Dynamics* 2, 133–143.
- Massaria, F., Sgavettib, M., Rioja, D., D'Alessandro, A., Prosserd, G., 1999. Composite sedimentary record of falling stages of Pleistocene glacio-eustatic cycles in a shelf setting (Crotone basin, south Italy). *Sedimentary Geology* 127, 85–110.
- Matsushima, Y., 1984. Shallow marine molluscan assemblages of postglacial period in the Japanese Islands—its historical and geographical changes induced by the environmental changes. *Bulletin of the Kanagawa Prefectural Museum* 15, 37–109 (Japanese with English and German abstract).
- Matsuura, N., 1996. Vertebrate fossils from the Omma Formation of Kanazawa area, Ishikawa Prefecture, Japan. *The Report of Hokuriku Geology Institute* 5, 55–88 (Japanese with English abstract).
- MuCubbin, D.G., 1982. Barrier island and strand plain facies. In: Scholle, P.A., Spearing, D. (Eds.), *Sandstone Depositional Environments*. American Association of Petroleum Geologists, Memoir 31, pp. 247–279.
- Mudelsee, M., Schulz, M., 1997. The mid-Pleistocene climate transition: onset of 100 ka cycle lags ice volume build-up by 280 ka. *Earth and Planetary Science Letters* 151, 117–123.
- Murakoshi, N., Masuda, F., 1992. Estuarine, barrier-island to strand-plain sequence and related ravinement surface developed during the last interglacial in the Paleo-Tokyo Bay, Japan. *Sedimentary Geology* 80, 167–184.
- Naish, T., 1997. Constraints on the amplitude of late Pliocene eustatic sea-level fluctuations: new evidence from the New Zealand shallow-marine sediment record. *Geology* 25, 1139–1142.
- Ogasawara, K., 1977. Paleontological analysis of Omma Fauna from Toyama-Ishikawa area, Hokuriku Province, Japan. *Science Reports of the Tohoku University, Second Series*. *Geology* 47, 43–156.
- Ohmura, I., Ito, T., Masaeda, H., Danbara, T., 1989. Magnetostratigraphy of the Omma Formation distributed in Kanazawa City, Ishikawa Prefecture, Central Japan. *Prof. H. Matsuo Mem.* pp. 111–124 (Japanese with English abstract).
- Pisias, N.G., Moore Jr., T.C., 1981. The evolution of Pleistocene climate: a time series approach. *Earth and Planetary Science Letters* 52, 450–458.
- Plint, A.G., 1988. Sharp-based shoreface parasequences and 'offshore bars' in the Cardium formation of Alberta; their relationship to relative changes in sea level. In: Wilgus, C.K., Hastings, B.S., Kendall, C.G.St.C., Posamentier, H.W., Ross, C.A., Van Wagoner, J.C. (Eds.), *Sea-Level Changes: An Integrated Approach*. Society of Economic Paleontologists and Mineralogists Special Publication 42, pp. 357–370.

- Plint, A.G., 1991. High-frequency relative sea-level oscillations in the Upper Cretaceous shelf clastics of the Alberta foreland basin: possible evidence for glacio-eustatic control? In: Macdonald, D.I.M. (Ed.) *Sedimentation, Tectonics and Eustasy*. International Association of Sedimentologist Special Publication 12, pp. 409–428.
- Plint, A.G., Norris, B., 1991. Anatomy of a ramp region sequence: facies successions, paleogeography and sediment dispersal patterns in the Muskiki and Marshybank Formations, Alberta foreland basin. *Bulletin of Canadian Petroleum Geology* 39, 18–42.
- Plint, A.G., Nummedal, D., 2000. The falling stage systems tract: recognition and importance in sequence stratigraphic analysis. *Geological Society Special Publication* 172, 1–18.
- Posamentier, H.W., Allen, G.P., James, D.P., Tesson, M., 1992. Forced regressions in a sequence stratigraphic framework: concepts, examples and exploration significance. *American Association of Petroleum Geologists Bulletin* 76, 1687–1709.
- Prell, W.L., 1982. Oxygen and carbon isotopic stratigraphy for the Quaternary of Hole 502B: evidence for two modes of isotopic variability. *Initial Reports of the Deep Sea Drilling Project* 68, 455–464.
- Ramm, M., Bjørlykke, K., 1994. Porosity/depth trends in reservoir sandstones: assessing the quantitative effects of varying pore-pressure, temperature history and mineralogy, Norwegian Shelf Data. *Clay Minerals* 24, 475–490.
- Raymo, M.E., Oppo, D.W., Curry, W., 1997. The mid-Pleistocene climate transition: a deep sea carbon perspective. *Paleoceanography* 12, 546–559.
- Raymo, M.E., Ruddiman, W.F., 1992. Tectonic forcing of late Cenozoic climate. *Nature*, 117–122.
- Raymo, M.E., Ruddiman, W.F., Froelich, P.N., 1988. Influence of late Cenozoic mountain building on ocean geochemical cycles. *Geology* 16, 649–653.
- Richards, D.A., Smart, P.L., Edwards, R.L., 1994. Maximum sea levels for the last glacial period from U-series ages of submerged speleothems. *Nature* 367, 357–360.
- Rio, D., Channell, J.E.T., Massari, F., Poli, M.S., Sgavetti, M., D'Alessandro, A., Prosser, G., 1996. Reading Pleistocene eustasy in a tectonically active siliciclastic shelf setting (Crotone peninsula, southern Italy). *Geology* 24, 743–746.
- Ruddiman, W.F., Raymo, M.E., Martinson, D.G., Clement, B.M., Backman, J., 1989. Pleistocene evolution: Northern hemisphere ice sheets and North Atlantic Ocean. *Paleoceanography* 4, 353–412.
- Saito, Y., 1989. Modern storm deposits in the inner shelf and their recurrence intervals, Sendai Bay, northeast Japan. In: Taira, A., Masuda, F. (Eds.), *Sedimentary Facies in the Active Plate Margin*. Terra Scientific Publishing Company, Tokyo, pp. 331–344.
- Sato, T., Takayama, T., 1992. A stratigraphically significant new species of the calcareous nannofossil *Reticulofenestra asanoi*. In: Ishizaki, K., Saito, T. (Eds.), *Centenary of Japanese Micropaleontology*. Terra Scientific Publishing Company, Tokyo, pp. 457–460.
- Sclater, J.G., Christie, P.A.F., 1980. Continental stretching: an explanation of the post Mid-Cretaceous subsidence of the central North Sea basin. *Journal of Geophysical Research* 85, 3711–3739.
- Shackleton, N.J., Bergeret, A., Peltier, W.R., 1990. An alternative astronomical calibration of the lower Pleistocene timescale based on ODP Site 677. *The Transactions of the Royal Society of Edinburgh-Earth Sciences* 81, 251–261.
- Takayama, T., Kato, M., Kudo, T., Sato, T., Kameo, K., 1988. Calcareous microfossil biostratigraphy of the uppermost Cenozoic formations distributed in the coast of the Japan Sea, Part 2: Hokuriku sedimentary basin. *Journal of the Japanese Association for Petroleum Technology* 53, 9–27.
- Trend-Staid, M., Prell, W.L., 2002. Sea surface temperature at the Last Glacial Maximum: a reconstruction using the modern analog technique. *Paleoceanography* 17 (17–1–17–18).
- Walker, R.G., Plint, A.G., 1992. Wave- and storm-dominated shallow marine systems. In: Walker, R.G., James, N.P. (Eds.), *Facies Models: Response to Sea Level Change*. Geological Association of Canada, pp. 219–238.